Probing Phase Structure and Location of Reverse Units in Poly(vinylidene fluoride) by Solid-State NMR

Catherine Hucher,[†] François Beaume,[†] René-Paul Eustache,[†] and Piotr Tekely*[,‡]

ARKEMA, Centre d'Etude de Recherche et Développement, 27470 Serquigny, France, and UMR CNRS 7565, Université H. Poincaré, 54506 Vandoeuvre-lès-Nancy, France

Received November 12, 2004; Revised Manuscript Received December 17, 2004

ABSTRACT: Investigation of phase structure of poly(vinylidene fluoride) and characterization of its NMR fingerprints from three main polymorphs are presented by exploiting ^{13}C-{^{19}F,^{1}H} and ^{19}F-{^{1}H} MAS NMR experiments. Selective excitation of ^{19}F NMR signal from different phases has been used for a straighforward identification and separation of spectroscopic signatures not only from the amorphous part but also from α, β, and γ polymorphs. A new insight into the phase structure of morphologically different samples has been gained by $T_{1\rho}(^{19}F)$ relaxation measurements in the conditions of very high spinning speeds and strong radio-frequency field. Motional heterogeneity of the reverse units has been revealed, and their spatial location in the amorphous, intermediate, and crystalline phases was quantified for the first time. The spectroscopic fingerprints along with phase structure features of PVF_2 and the ways exploited in this work for their retrieval might be useful to obtain structural information on PVF_2 of different origin as well as on other types of fluoropolymers.

Introduction

Poly(vinylidene fluoride) (PVF_2) shows outstanding piezo- and pyroelectric properties, extremely convenient processability, and excellent mechanical characteristics.[1] PVF_2 is usually produced by the free-radical suspension or emulsion polymerization, the increasing temperature of polymerization leading to the increasing incidence of reverse monomeric units. Tail-to-tail (T−T) units generally follow head-to-head (H−H) units immediately and occur to the same extent. Such inverted monomeric units generally account for 3.5−8% of the polymer chain and affect strongly molecular conformations in the crystalline phase and the crystallization of various polymorphs as well as the mechanical properties of this polymer.[2]

The extraordinary electric properties ranging from dielectric to ferroelectric material stem from the crystalline structure of PVF_2. Several crystalline phases have been reported.[3] The most common α-polymorph occurs in all melt-quenched samples and is nonpolar because of antiparallel packing of chains having a distorted TG^+TG^- conformation without steric strains between fluorine atoms.[3a] The β-PVF_2, all-trans planar zigzag conformation along the chain backbone,[3b] is the most important polymorph due to its high piezoelectric coefficient and is easily obtained by streching melt-crystallized films. The as-cast γ-PVF_2 has essentially the $T_3G^+T_3G^-$ conformation.[3c] This form is also polar and can be obtained from solution deposition or by heat treatment of the α-form inducing the changes in the molecular conformation from TG^+TG^- to $T_3G^+T_3G^-$ by flip-flop motions.[3]

Various manufacturing, storage, or use conditions can influence the total crystalline content, convert some polymorphs into others, or change their ratios in the initial material.[1,2,4] This can lead to the significant changes of their electric and/or mechanical properties, and a clear identification of the presence and the amount of different polymorphs is frequently of prime importance. In this work we will show that such an information can be gained by exploiting high-resolution ^{19}F and ^{13}C NMR spectroscopy. Phase structure of morphologically different samples along with the spatial location of the reverse units will be also probed.

Experimental Part

Polymers. Three different types of semicrystalline PVF_2 samples, manufactured by Atofina, France, and containing pure α, mixed ($\alpha + \beta$), or ($\alpha + \gamma$) polymorphs, were investigated in this work. They correspond to the following thermomechanical histories: (i) sample **1** having a pure α phase obtained by natural cooling in air from the melt state; (ii) sample **2** with mixed ($\alpha + \beta$) polymorphs and obtained from sample **1** after extensive drawing; (iii) sample **3** with mixed ($\alpha + \gamma$) polymorphs obtained from sample **1** after several successive annealings at increasing temperatures in the range 150−170 °C.

Each sample was cut into small pieces to fill the NMR rotors.

Solid-State NMR Experiments. All experiments were carried out on a Bruker DSX 300 spectrometer. The operating frequencies were 300.13 MHz for ^{1}H and 282.5 MHz for ^{19}F. Different pulse sequences have been used in this work. ^{19}F-{^{1}H} magic-angle spinning (MAS) spectra have been recorded at a spinning frequency of 30 kHz and applying a pulse sequence for suppression of the background signal from the probe.[5] T_2 or $T_{1\rho}$ relaxation filters have been applied for selective elimination of the NMR signals from crystalline and amorphous phases, respectively. For selective excitation of ^{19}F NMR signal from different polymorphs we used a SELDOM pulse train.[6] The high-power proton TPPM[7] or XiX[8] decoupling scheme with the radio-frequency field strength of 120 kHz has been systematically applied. ^{13}C-{^{19}F,^{1}H} CP/MAS spectra have been recorded at a spinning frequency of 30 kHz by cross-polarization transfer of magnetization from the fluorine spin system and in the presence of simultaneous high-power phase-modulated decoupling on both the proton and fluorine channels with the field strength of 120 kHz.

Results and Discussion

Separating Spectral Signatures from the Amorphous and Crystalline Phases. *High-Resolution ^{19}F-*

† ARKEMA.
‡ Université H. Poincaré.
* Corresponding author: e-mail Piotr.Tekely@rmn.uhp-nancy.fr; Fax (33) 383684347; Tel (33) 383684352.

10.1021/ma0476700 CCC: $30.25
Published on Web 02/04/2005

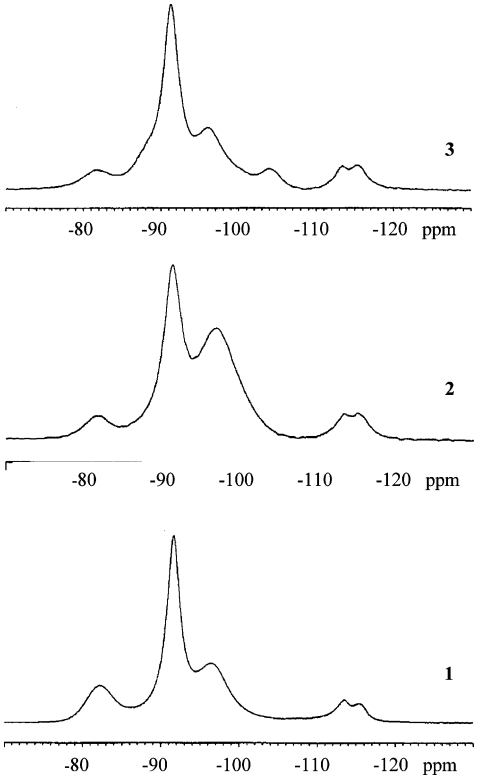

Figure 1. Directly polarized ^{19}F-{^{1}H} MAS NMR spectra of three morphologically different semicrystalline samples of PVF_2. All spectra have been recorded using high power proton decoupling and magic angle spinning at a frequency of 30 kHz.

{^{1}H} Spectra. Figure 1 shows the ^{19}F NMR spectra of three morphologically different PVF_2 samples recorded under high-power proton decoupling and high frequency of magic-angle spinning. Several resonance signals on a chemical shift scale are clearly resolved. To separate the signals from the amorphous and crystalline phases, the easiest way is to take advantage of their different molecular mobility on a kilohertz time scale or of their different homonuclear dipolar interactions.[9] This can be easily done on a PVF_2 powder sample by an efficient elimination of fluorine resonances from the amorphous part when applying a standard spin-lock procedure ($T_{1\rho}$ filter) or by a selective suppression of signals from the crystalline regions using a delayed (spin echo) acquisition (T_2 filter). As shown in Figure 2, for the sample under investigation having the crystalline phase present exclusively in the α form, the crystalline only spectrum reveals two fully separated resonance signals at −82 and −97 ppm, resulting from the magnetic inequivalence of fluorines in the trans−gauche conformation.[10] On the contrary, the amorphous only spectrum contains a dominant signal at −91 ppm close to that of the main chain fluorine signal observed in the liquid-state spectra.[11] The presence of two minor high field signals (5−7% of total spectral intensity in agreement with 4.5% head-to-head defect content estimated from solution state ^{19}F NMR) between −113 and −116 ppm is assigned to inverted monomeric units.[11] The spatial emplacement of these reverse units in different phases is the subject of detailed examination presented in the second part of this paper.

More complex spectra of crystalline components (after elimination of resonances from the amorphous part by proton $T_{1\rho}$ filter) are observed for PVF_2 samples having crystalline phase composed with mixed polymorphs.

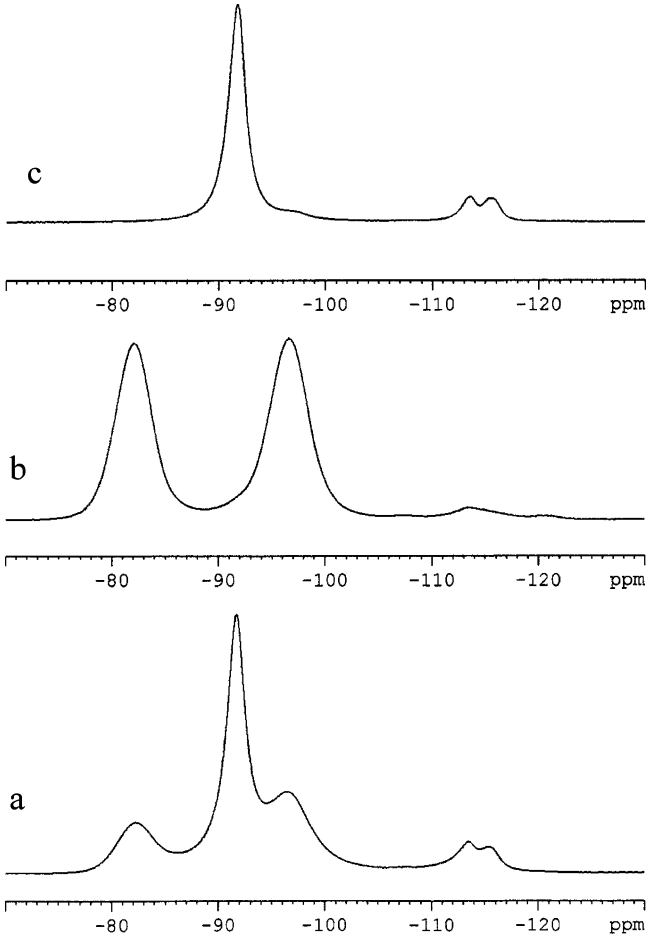

Figure 2. ^{19}F-{^{1}H} MAS NMR spectra of sample **1** having the crystalline phase present in the α form only. (a) Total spectrum. (b) Spectrum of the crystalline component recorded by using the $T_{1\rho}(^{19}F)$ filter (spin-lock period of 40 ms). (c) Spectrum of the amorphous component recorded by using the $T_2(^{19}F)$ filter $\tau-\pi-\tau$ (τ = 40 μs). For better visualization, all spectra are shown with the same intensity.

Figure 3 shows that such spectra show either two or five signals of different amplitude. To separate the resonance signals from different polymorph, we have selectively excited the resonance signals from the α form. To do so, we apply additionally a selective excitation by a SELDOM pulse train with a frequency carrier placed at the resonance position of signal to be selectively excited.[6] The sequence begins with a nonselective $\pi/2$ pulse used to convert the entire transverse magnetization into longitudinal magnetization. The selective excitation is then obtained by an application of a pulse train of the form $[\pi/2_x-\tau_1-\pi/2_{-x}-\tau_2]_N$. It starts with a $\pi/2_x$ pulse followed by a first period τ_1 during which the magnetization evolves mainly under the influence of the chemical shift. The second $\pi/2_{-x}$ pulse brings back the individual magnetization vectors into the *xz* plane. During a second τ_2 the decoupling of protons is switched off, and the transverse components of magnetization vectors vanish while the remaining longitudinal magnetization enters into the flip-flop spin exchange. Repeating N times this sequence leads to efficient disappearance of resonance signals from all parts of the spectral region except those located near the carrier frequency and those to which the selected magnetization migrated during the spin diffusion exchange. As shown in Figure 3, when placing the carrier frequency at the position of low field resonance signal from the α form,

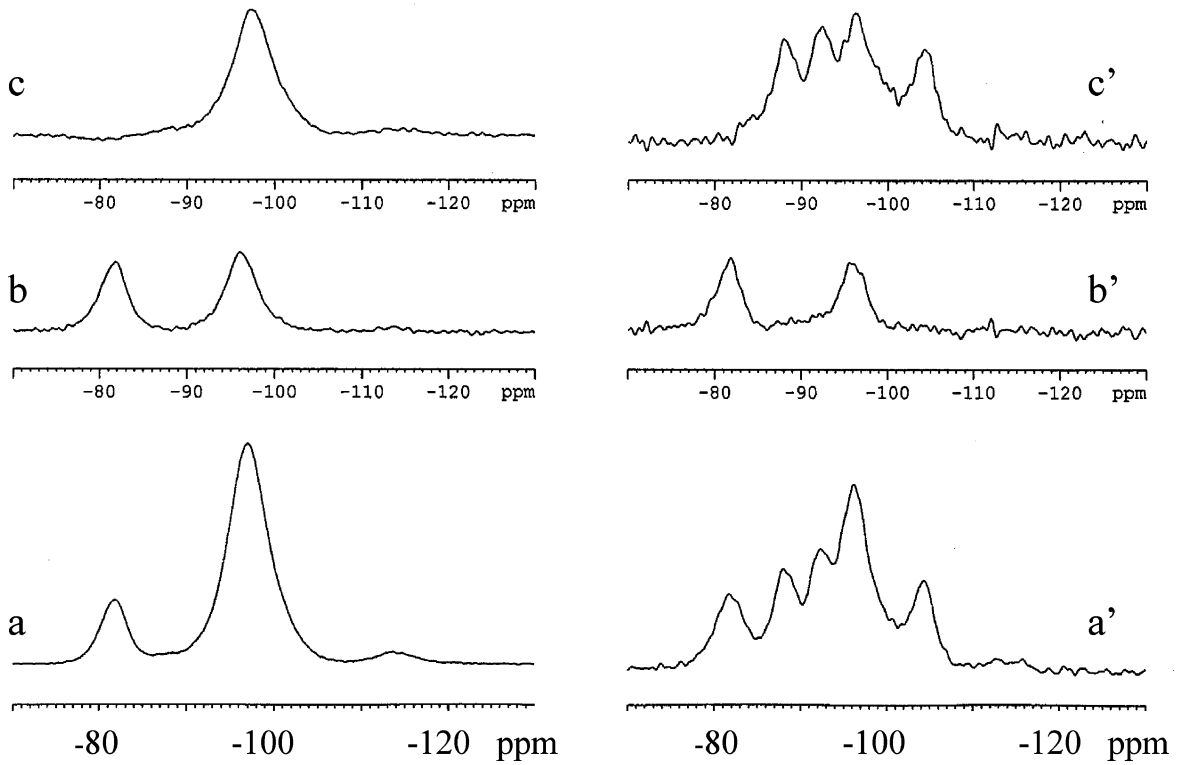

Figure 3. (a, a′) ^{19}F-{^{1}H} MAS NMR spectra of crystalline components in samples **2** and **3** having mixed polymorphs. Both spectra have been recorded after using the $T_{1\rho}(^{19}F)$ filter (SL = 40 ms). (b, b′) Selectively excited resonance signals of the α polymorph by an additional application of a SELDOM pulse train (τ_1 = 60 μs, τ_2 = 2 ms, N = 8). (c, c′) Separated resonance signals of β and γ polymorphs, respectively, obtained by corresponding spectral subtraction.

the spin-exchange between fluorines belonging to this phase leads to the selective excitation of both α form peaks in each sample. The subtraction of such spetra from the total spectrum of the crystalline part reveals spectral features of the remaining crystalline forms having a single resonance peak at −97 ppm for the first sample and four resonance signals at −88, −92.5, −96.5, and −104.2 ppm for the second sample. The single resonance peak gives immediately evidence of the all-trans conformation in the β form,[10] while four peaks visualize nicely the spectral fingerprint of $T_3G^+T_3G^-$ conformation in the γ form.[12] This allows independent observation of resonance signals from different components in PVF_2 powder samples endowed with mixed α, β, and γ polymorphs and their quantification by spectral subtraction without any assumption about their line shapes. Albeit the spectral deconvolution from the known positions of corresponding fingerprints can also be envisaged, such a way of quantification of the relative amounts of polymorphs has to be applied prudently due to only partially justified Lorentzian or mixed line shapes of individual distributions of chemical shift positions and possible imbalance of two resonance signals in the α phase. For the same reasons, the spectral decomposition will be even more difficult with respect to the amorphous or rigid noncrystalline components.

^{19}F Chemical Shift Anisotropy Fingerprints of the α Polymorph. Solid-state measurements permit an easy access to the principal values of chemical shift anisotropy (CSA) tensors.[13] The chemical shielding interaction is indeed of prime interest for chemists involved in the study of molecular structure or dynamics and is appropriately described by a tensor whose nature depends on the local electronic environment of the nucleus and its local site symmetry. In solution, the molecular tumbling averages out the spectral features due to the anisotropic part of the chemical shielding tensor, leaving its isotropic part $\delta_{iso} = (\delta_{11} + \delta_{22} + \delta_{33})/3$, and where δ_{ii} are three principal elements of the chemical shift tensor. As shown above, a rapid magic-angle spinning of powder solids also leads to an averaged isotropic value for a given resonance. However, by virtue of their nature, the principal components are more sensitive to the changes in the electronic environment which itself may be influenced by the conformational effects.[14]

Su and Tzou[15] were first to make an attempt to retrieve the ^{19}F chemical shift principal values in α form of PVF_2. They reported that the two peaks from the crystalline phase have significantly different shielding anisotropies. However, because of the presence of motionally averaged amorphous signal, partially superposing with a high field crystalline peak, the extracted values appear of unsufficient precision to give credence to such a difference. To create more favorable conditions for recovering of CSA parameters of crystalline peaks, we have recorded ^{19}F MAS spectra by using $T_{1\rho}$ filter for selective suppression of the amorphous signal (see above) at a moderate spinning frequency of 15 kHz. As shown in Figure 4, this permits to get two well-separated families of spinning sidebands, which can be now properly analyzed by numerical simulations. Because of the presence of homonuclear dipolar couplings between fluorines, a possible additional contribution of this interaction to the spinning sidebands also needs to be considered. For this, we have simulated dipolar only spectrum dominated by dipolar interactions within CF_2 groups (r_{F-F} = 2.14 Å corresponding to the dipolar coupling constant of 10.86 kHz). Although a small number of the interchain distances between fluorines

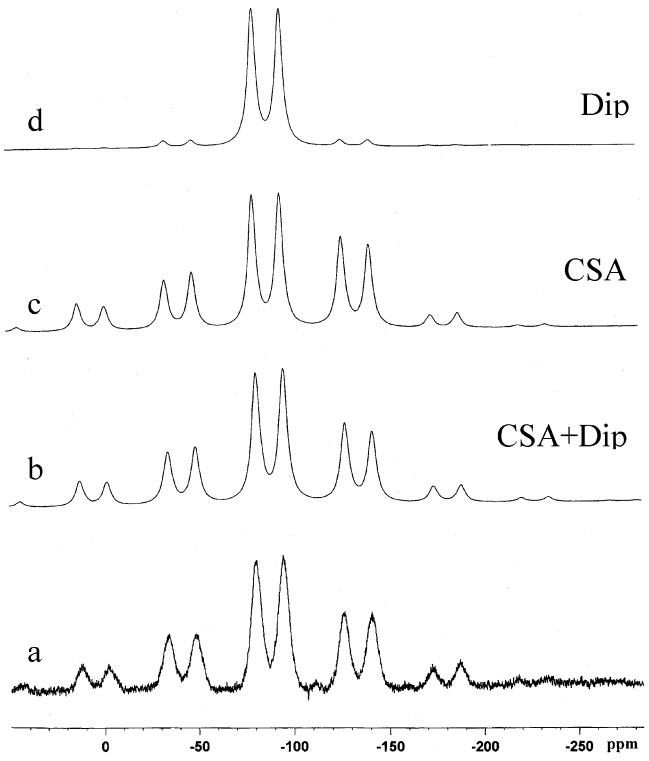

Figure 4. ^{19}F MAS NMR spectra of crystalline phase in the α form: (a) experimental spectrum; (b) simulated spectrum including chemical shift anisotropy and dipolar interactions; (c) simulated chemical shift anisotropy, and (d) dipolar only spectra. In all cases the spinning frequency was 15 kHz.

in the α polymorph[3] can be as short as 1.568 Å, which corresponds to the dipolar strength of 27.6 kHz, we consider that the small fraction of fluorines involved in such short distances is unable to contribute significantly to the observed spinning sidebands. Independent T_2 spin-echo and double-quantum experiments (not shown) fully corroborate such a hypothesis. Consequently, as visualized in Figure 4 (top), the dipolar contribution to the spinning sidebands is quite small, yet can slightly modify the ratio of intensities within the spinning sidebands manifolds. This prompted us eventually to fit the experimental spectrum in Figure 4 by assuming a simultaneous presence of both types of internal interactions. The principal elements δ_{ii}, anisotropy ($\Delta\delta$), asymmetry (η), span (Ω), and skew (κ) parameters of

Table 1. Experimental ^{19}F Values of the Principal Tensor Elements δ_{ii} and Corresponding Anisotropic Parameters for CF_2 Groups in α Form of PVF_2[a]

	δ_{iso} (ppm)	δ_{11} (ppm)	δ_{22} (ppm)	δ_{33} (ppm)	$\lvert\Delta\delta\rvert$ (ppm)	Ω (ppm)	η	κ
1	−81.8	29	−115	−159	166	188	0.40	−0.53
2	−96.1	10	−115	−183	159	193	0.64	−0.29

[a] Estimated errors in δ_{11}, δ_{22}, and δ_{33} are ±4 ppm; span is expressed as $\Omega = \delta_{11} - \delta_{33}$, skew as $\kappa = 3(\delta_{22} - \delta_{iso})/\Omega$; anisotropy is calculated as $\Delta\delta = {}^3/_2(\delta_{11} - \delta_{iso})$ and asymmetry as $\eta = (\delta_{22} - \delta_{33})/(\delta_{11} - \delta_{iso})$.

the ^{19}F CSA tensors for the two crystalline peaks were derived from the iterative calculations of corresponding spinning sideband manifolds. The fitted values of the principal tensor elements δ_{ii} along with corresponding anisotropic parameters are given in Table 1. The difference in the shape of the chemical shift anisotropy of the two crystalline peaks is depicted in Figure 5. Contrary to earlier published data,[15] the results reveal almost identical anisotropy and span parameters of both peaks. This is indeed what one would expect for chemically equivalent but magnetically inequivalent CF_2 groups. More interesting, significant differences, which we assign mainly to conformational effect, appear for the asymmetry and skew parameters.

High-Resolution ^{13}C-{^1H,^{19}F} Spectra. The double decoupled ^{13}C CP/MAS spectrum of PVF_2 sample containing the α form is shown in Figure 6. Two intense resonance peaks at 43.0 and 121.8 ppm represent the CH_2 and CF_2 groups, respectively. Further three minor peaks, centered around 22, 29, and 38 ppm, are the "defect" resonances of reversed monomer units reported first in the liquid-state spectra.[16] According to earlier observations,[17] both ^{1}H to ^{13}C and ^{19}F to ^{13}C cross-polarization provide equivalent spectra except for small differences in intensity of two peaks caused by different heteronuclear distances.

To gain an insight into spectral features from different crystalline modifications, we have recorded the ^{13}C spectra of each sample (Figure 7) by using the $T_{1\rho}$ (^{19}F) filter preceding the cross-polarization ^{19}F → ^{13}C transfer. This allows an efficient elimination of resonance signals from carbons placed in the amorphous phase and reveals significant differences between different crystalline forms, especially for CH_2 group. This group shows indeed 1, 2, and 3 resonance signals for pure α, (α + β),

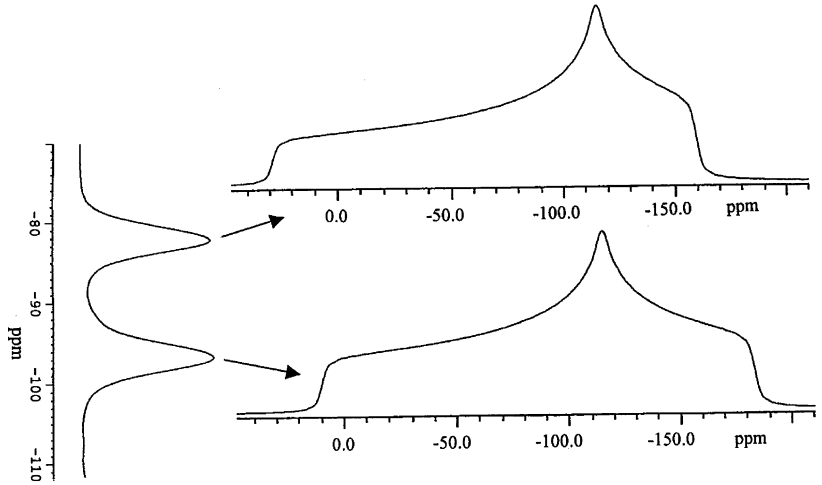

Figure 5. ^{19}F chemical shift anisotropy spectra of the two crystalline peaks having the isotropic chemical shifts at −81.8 ppm (top) and −96.1 ppm (bottom).

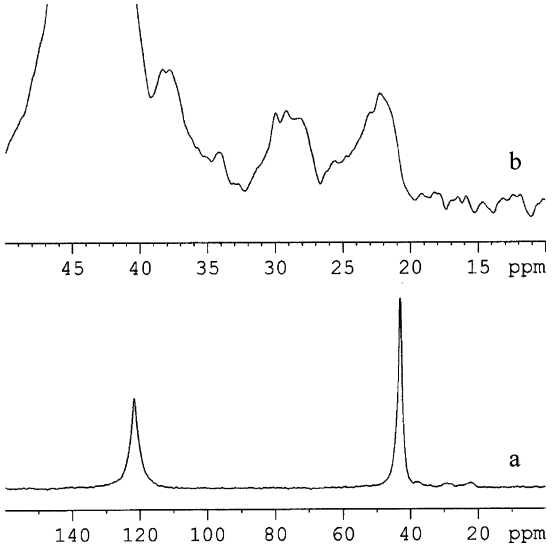

Figure 6. (a) Proton and fluorine decoupled ^{13}C CP/MAS spectrum of PVF_2 sample **1** containing the α form. (b) "Defect" resonances of reversed monomer units. MAS: 10 kHz, contact time 3 ms.

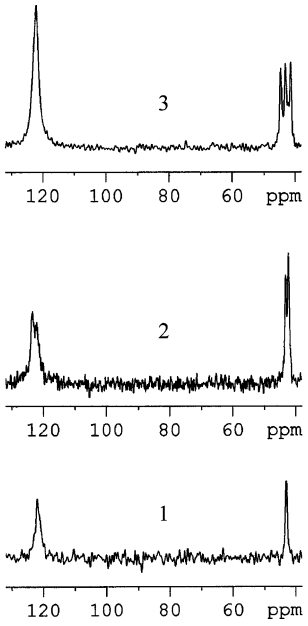

Figure 7. Double decoupled ^{13}C CP/MAS spectra of crystalline components in samples containing α (**1**), α and β (**2**), and α and γ (**3**) polymorphs recorded by using the $T_{1\rho}(^{19}F)$ filter (spin-lock period of 40 ms). MAS: 10 kHz, contact time 3 ms.

and ($\alpha + \gamma$) forms, respectively. This suggests immediately that the α and β forms are represented by a single resonance peak at 43.0 and 42.1 ppm, respectively, while the γ form reveals two main resonance peaks at 41.3 and 44.5 ppm. Such an assignment was checked in a rather demanding experiment based on the selective excitation of ^{19}F magnetization from the α polymorph (see above) and its efficient transfer to the ^{13}C spin system within the same crystalline form. It is worth pointing out that this challenging transfer can only be considered at very high spinning speed, guaranteeing a reasonable amount of selectively excited magnetization due to efficient suppression of spinning sidebands which in turns implies the need for a great accuracy in experimental conditions of cross-polarization procedure ($n = \pm 1$ Harmann−Hahn conditon) and

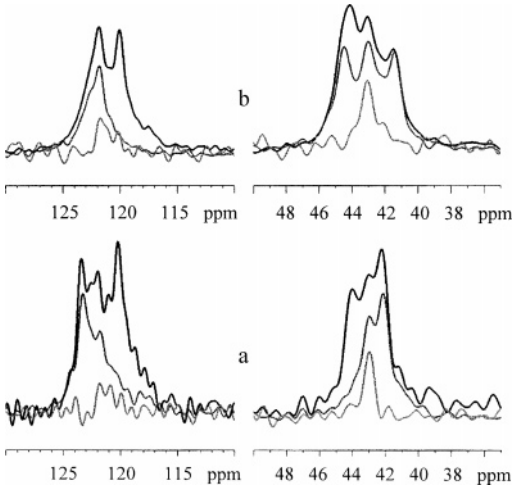

Figure 8. Selective excitation of resonance signals from the α form in ^{13}C CP/MAS spectra of PVF_2 samples containing α and β (a) and α and γ (b) polymorphs. Crystalline only spectra have been recorded by using the $T_{1\rho}(^{19}F)$ filter (spin-lock period of 40 ms). MAS: 30 kHz, contact time 3 ms. The spectra of decreasing intensity correspond respectively to the total, crystalline only and α-form only resonances.

particularly severe double decoupling requirements. As shown in Figure 8, this experiment provides indeed unambiguous proves of different ^{13}C fingerprints from corresponding polymorphs.

Spatial Location of the Reverse Units. As mentioned above, the inverted monomeric units in PVF_2 can affect strongly molecular conformations in the crystalline phase and the crystallization of various polymorphs.[1,18] The piezo- and pyroelectrical properties of the β polymorph can also be affected by the presence of the reverse units. It has been shown, for example, that the α/β ratio and the mechanical and electrical properties of the material depend on the mole percentage of the reverse units.[19] So far, only a few papers reported on the spacial location of these units in PVF_2. From the observation of isothermal thickening and the dependence of the heat of fusion on H−H defect content, Chen and Frank suggested that the reverse units could be incorporated into the lamellar region.[18] Nandi and Mandelkern investigated the influence of chain structure on the equilibrium melting temperature of PVF_2 and also concluded that the H−H units could enter the crystalline lattice.[20] More recently, etched samples of PVF_2 in the α form indicated that the distribution of defects between the crystalline and amorphous portion varied from 0.7 to 0.9.[21] On the other hand, from the solid-state NMR experiments Ando et al.[22] concluded that the content of regioirregular sequences in the crystalline domain of PVF_2 was negligible, which corroborated with earlier observations of Scheler[23] that the reverse units had a spin exchange with the amorphous region only. The results reported very recently by Wormald et al.[24] also showed the majority of reverse units to be relatively mobile (i.e., amorphous); however, their presence in relatively rigid domains was also suggested. This is definitely the case of all three samples under investigation in this work, for which, as revealed by T_2 and $T_{1\rho}$ filtrated spectra, the reverse units are endoved with a large gradient of mobility, the majority of them belonging to the mobile amorphous phase. This last evidence is clearly confirmed in spin diffusion experiments showing a preferential flow of selectively excited magnetization from the reverse units to the

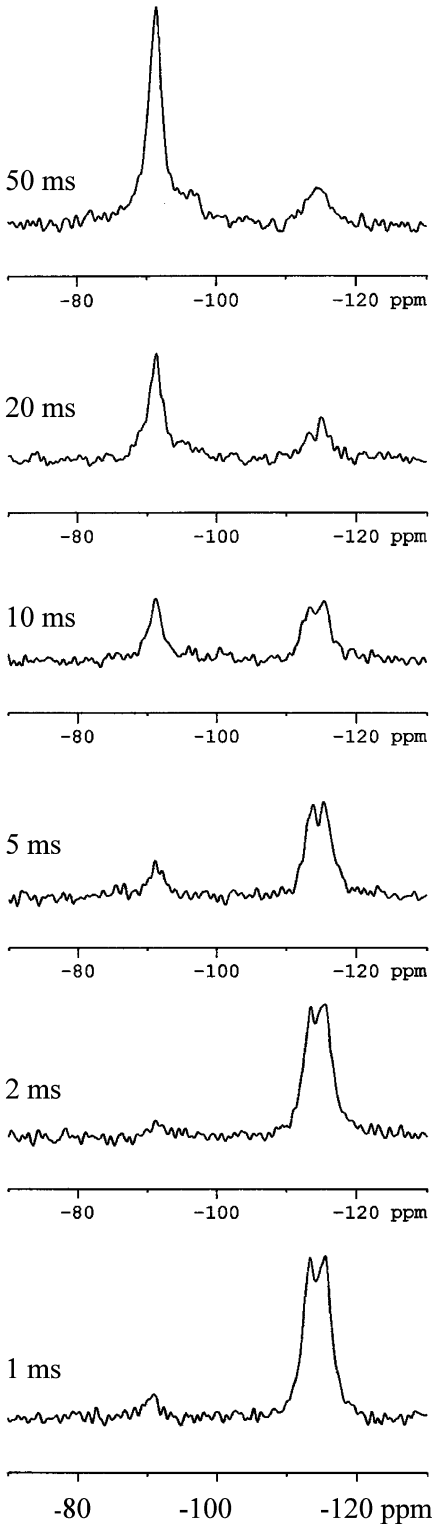

Figure 9. ^{19}F spectra of PVF_2 sample **2** with mixed α and β polymorphs recorded for different times of spin-diffusion flow of fluorine magnetization from selectively excited reverse units to the main units. SELDOM pulse train has been used to prepare the initial gradient of magnetization. All spectra have been recorded using high power proton decoupling and magic angle spinning at a frequency of 30 kHz.

main units located in the amorphous part (Figure 9).

To get a more quantitative insight into the spacial location of reverse units and the phase structure of samples under investigation, we have analyzed the temporal evolution of the integrated intensity of fluorine-19 resonance signals from the reverse H−H:T−T units

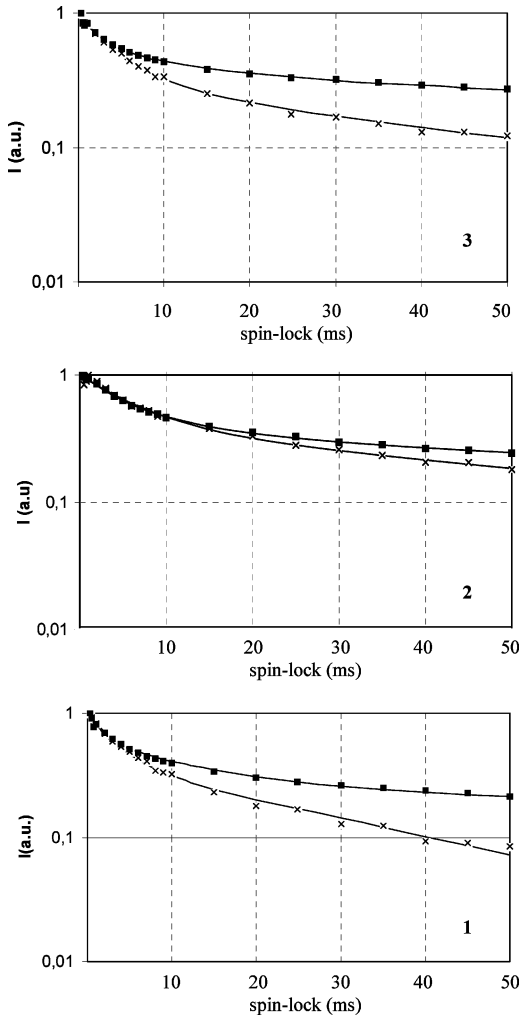

Figure 10. Spin-lock time dependence of the ^{19}F magnetization in the reverse (×) and main units (■) for PVF_2 samples with crystalline phase in the α-form (**1**), the mixed α and β forms (**2**), and the mixed α and γ forms (**3**). MAS: 30 kHz, spin-lock ν_{rf} = 125 kHz.

and from main H−T units in the rotating frame relaxation measurements with spin-lock time extending up to 50 ms and in the presence of high spin-lock rf field strength and very high spinning speeds (Figure 10). In all cases but one, for satisfactory fitting of the experimental decays, the presence of three exponential relaxation processes had to be assumed. A simple or two-exponential decay forms were found to be unable to describe finely the decaying magnetizations on such a long time scale. The fitted relaxation parameters and the percentage of each component are given in Table 2.

The data as a whole reveal the phase structure of each sample consisting in the presence of three components of decreasing mobility, which according to a commonly accepted phase structure of semicrystalline polymers are assigned to the amorphous (mobile), interphase (motionally restricted, most probably mainly from the chains on the surfaces of crystalline lamellae), and crystalline (rigid) phases. Two salient features of data from Table 2 for the main H−T units and the reverse units are presented schematically in Figure 11. Somewhat unexpectedly, both of them show symmetrically opposite trends of the amount of intermediate and rigid components and a constant amount of the mobile components. For main units this clearly shows up that when going from sample with pure α form to samples

Table 2. Phase Structure Composition and Spacial Location of Reverse Units in Mobile, Intermediate, and Rigid Components As Revealed by ^{19}F $T_{1\rho}$ Relaxation Measurements of Main H−T and Reverse H−H:T−T Units in PVF_2

location/phase structure[a]		main units		reverse units[b]	
		$T_{1\rho}$ (ms)	%[c]	$T_{1\rho}$ (ms)	%[c]
	M	1.2	38	3.4	61
	I	10.0	35	29.7	39
α	R	≥150.0	27		
	M	4.0	40	6.4	65
	I	11.5	28	55.0	35
α + β	R[d]	≥150.0	32	≥150.0	5
	M	2.0	38	4.0	64
	I	9.7	25	30.0	27
α + γ	R[e]	≥150.0	37	≥150.0	9

[a] M = mobile, I = intermediate, R = rigid. [b] 5−7% of total spectral intensity. [c] Estimated error is ±3%. [d] 30% of the α form, 70% of the β form. [e] 40% of the α form, 60% of the γ form.

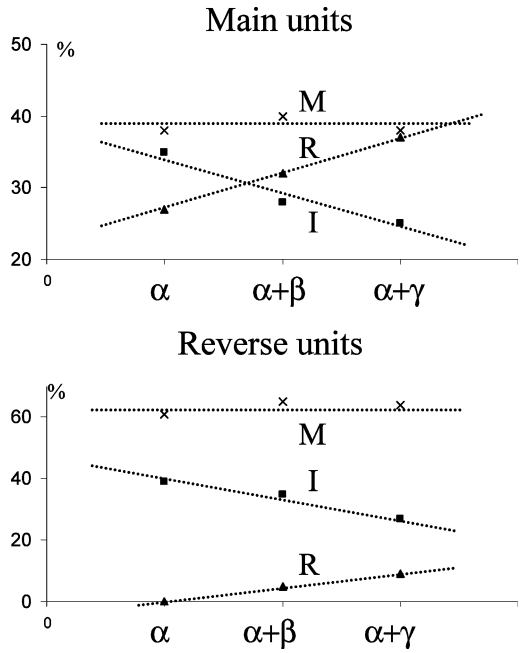

Figure 11. Amount of the mobile (M, ×), intermediate (I, ■), and rigid (R, ▲) components in the main and reverse units for PVF_2 samples with different polymorphs.

with mixed polymorphs, besides a partial transformation of the α to β and γ forms, the observed total increase of the amount of the most rigid (crystalline) phases occurs exclusively at the expense of the intermediate phase. Equally interesting, though as expected from spin diffusion spectra shown in Figure 9, the majority of the reverse units is systematically located in the most mobile (amorphous) part; a significant proportion of them is located in the intermediate component, which in turn can convert to the most rigid (crystalline) phase for both samples with mixed polymorphs. Indeed, the results strongly suggest that the α polymorph does contain negligible pourcentage, if any, of the reverse units, while about 5 and 9% of such units are included in β and γ polymorphs, respectively. Corroborating experimental evidence of these structural features is provided by the selective excitation of fluorine magnetization from individual polymorphs in sample with mixed α and γ forms. In fact, as visible in Figure 12, the selective excitation of resonance signals from the α form does not lead to any simultaneous excitation of resonances from the reverse units. On the contrary, the

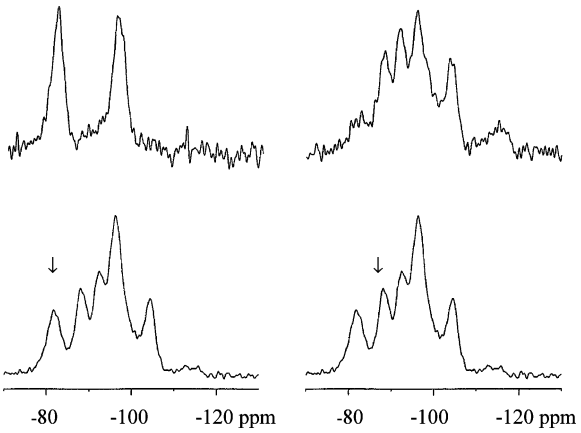

Figure 12. Selective excitation of resonance signals in α (left) and γ (right) polymorphs by a SELDOM pulse train applied at two different carrier frequencies (↓).

resonance signals of the reverse units clearly appear during selective excitation of magnetization from the γ form as one would expect assuming their spatial closeness. This is indeed an another strong indication for a significant pourcentage of the reverse units belonging to the crystalline phase of the γ polymorph.

Conclusions

We have shown that it is possible to unequivocally assign specific ^{13}C and ^{19}F NMR fingerprints from three main α, β, and γ polymorphs of PVF_2 by exploiting ^{13}C-{^{19}F,^{1}H} and ^{19}F-{^{1}H} MAS NMR experiments. This includes the first solid-state NMR results reported for ^{13}C signatures of PVF_2 from different polymorphs. The obvious advantage of solid-state NMR in a straightforward identification and quantification of different polymorphs as compared with other types of date like DSC or X-ray is due to the presence of simple and well-separated fingerprints available from a single NMR spectrum. Moreover, in contrast to other methods, the characteristic spectral features of each polymorph are not sensitive to the thickness of crystalline lamellas or their imperfections, and the quantification of corresponding amounts does not need any use of reference samples.

Phase structure of three samples has been probed by $T_{1\rho}(^{19}F)$ relaxation measurements and revealed that when going from sample with pure α form to samples with mixed polymorphs, the observed total increase of the amount of crystalline phase occurred only at the expense of the intermediate phase. New insights into the spatial location of the reverse units has been presented. Although the majority of the reverse units was found located in the most mobile (amorphous) part, a significant proportion was also detected in the intermediate component, which in turn converted to the crystalline phase for both samples with mixed polymorphs. The spectroscopic fingerprints and phase structure features of PVF_2 as well as the ways exploited in this work for their retrieval will be useful to obtain structural information on PVF_2 of different origin and on other types of fluoropolymers.

References and Notes

(1) Lovinger, A. J. Poly(Vinylidene Fluoride). In *Developments in Crystalline Polymers-1*; Basset, D. C., Ed.; Elsevier Applied Science Publishers: Amsterdam, 1982; Vol. 1, pp 195−273 and references therein.

(2) Wang, T. T.; Herbert, J. M.; Glass, A. M. *The Application of Ferroelectric Polymers*; Chapman and Hall: New York, 1987.
(3) (a) Takahashi, Y.; Matsubara, Y.; Tadokoro, H. *Macromolecules* **1983**, *16*, 1588−1592 and references therein. (b) Takahashi, Y.; Tadokoro, H.; Odajima, A. *Macromolecules* **1980**, *13*, 3, 1318−1320. (c) Takahashi, Y.; Tadokoro, H. *Macromolecules* **1980**, *13*, 1317−1318.
(4) (a) Benz, M.; Euler, W. B. *J. Appl. Polym. Sci.* **2003**, *89*, 1093−1100. (b) Neidhöfer, M.; Beaume, F.; Ibos, L.; Bernès, A.; Lacabanne, C. *Polymer* **2004**, *45*, 1679−1688. (c) Esterly, D. M.; Love, B. J. *J. Polym. Sci., Part B: Polym. Phys.* **2004**, *42*, 91−97.
(5) Cory, D. G.; Ritchey, W. M. *J. Magn. Reson.* **1988**, *80*, 128−131.
(6) Tekely, P.; Brondeau, J.; Elbayed, K.; Retournard, A.; Canet, D. *J. Magn. Reson.* **1988**, *80*, 509−516.
(7) Bennett, A. E.; Rienstra, C. M.; Auger, M.; Lakshmi, K. V.; Griffin, R. G. *J. Chem. Phys.* **1995**, *103*, 6951−6958.
(8) (a) Tekely, P.; Palmas, P.; Canet, D. *J. Magn. Reson. A* **1994**, *107*, 129−133. (b) Detken, A.; Hardy, E. H.; Ernst, M.; Meier, B. H. *Chem. Phys. Lett.* **2002**, *356*, 298−304.
(9) McBrierty, V. J.; Packer, K. J. *Nuclear Magnetic Resonance in Solid Polymers*; Cambridge University Press: New York, 1993.
(10) Holstein, P.; Scheler, U.; Harris, R. K. *Polymer* **1998**, *39*, 4937−4941.
(11) Ferguson, R. C.; Brame, Jr., E. G. *J. Phys. Chem.* **1979**, *83*, 1397−1401.
(12) Park, J. W.; Seo, Y. A.; Kim, I.; Ha, X. S.; Aimi, K.; Ando, S. *Macromolecules* **2004**, *37*, 429−436.
(13) Schmidt-Rohr, K.; Spiess, H. W. *Multidimensional Solid-State NMR and Polymers*; Academic Press: New York, 1994.
(14) Harper, J. K.; Grant, D. M. *J. Am. Chem. Soc.* **2000**, *122*, 3708−3714.
(15) Su, T.-W.; Tzou, D.-L. M. *Polymer* **2000**, *41*, 7289−7293.
(16) Bovey, F. A.; Schilling, F. C.; Kwei, T. K.; Frisch, H. L. *Macromolecules* **1977**, *10*, 559−561.
(17) Holstein, P.; Scheler, U.; Harris, R. K. *Magn. Reson. Chem.* **1997**, *35*, 647−649.
(18) Chen, L. T.; Frank, C. W. *Ferroelectrics* **1984**, *57*, 51−62.
(19) Lovinger, A. J.; Davis, D. D.; Cais, R. E.; Kometani, J. M. *Polymer* **1987**, *28*, 617−626.
(20) Nandi, A. K.; Malderkern, L. *J. Polym. Sci., Part B: Polym. Phys.* **1991**, *29*, 1287−1297.
(21) Dikshit, A. K.; Nandi, A. K. *J. Polym. Sci., Part B: Polym. Phys.* **2000**, *38*, 297−308.
(22) Ando, S.; Harris, R. K.; Reinsberg, S. A. *Magn. Reson. Chem.* **2002**, *40*, 97−106.
(23) Scheler, U. *Bull. Magn. Reson.* **1999**, *19*, 52.
(24) Wormald, P.; Apperley, D. C.; Beaume, F.; Harris, R. K. *Polymer* **2003**, *44*, 643−651.

MA0476700